

UNITARY MULTIPERIPHERAL MODELS*

S. Auerbach, R. Aviv and R. Sugar

Department of Physics, University of California, Santa Barbara, California 93106

and

R. Blankenbecler

Stanford Linear Accelerator Center, Stanford University, Stanford, California 94305

ABSTRACT

The method of constructing unitary S-matrices developed in a recent paper is generalized and applied to two versions of the multiperipheral model. In these models the standard perturbation expansion of the S-matrix diverges, so an alternative expansion with improved convergence properties is developed. It is shown that the unitarity condition generates a new type of cut in the angular momentum plane which is dynamical in origin in contrast to the essentially kinematical Mandelstam cuts. This new type of cut insures that the Froissart bound on the total cross section is obeyed. In an exactly solvable model it is shown that the contribution of the multiregge region of phase space to the total cross section always decreases as a power of the energy if the input Regge trajectory is one or less. It is argued that the qualitative features of the models discussed here will hold for a wide class of multiperipheral-like models.

* Work supported in part by the U. S. Atomic Energy Commission and the National Science Foundation.

I. INTRODUCTION

In order to discuss diffraction scattering and particle production at high energies it is essential to take into account the constraint of multiparticle unitarity. In a recent paper¹ a class of solvable models was constructed for which the multiparticle S-matrix is exactly unitary at high energies.² As in the multiperipheral model, it is assumed that particles are produced and absorbed from chains; however, in order to satisfy unitarity it is essential to take into account diagrams, such as those shown in Figure 1, in which production takes place from more than one chain. In I we considered a class of models in which only one particle is created or destroyed on each chain. In the present paper we generalize our results to include chains from which an arbitrary number of particles can be created or destroyed.

The classic multiperipheral and multiregge models have well-known difficulties with unitarity which can lead to violations of the Froissart bound.³ This problem can be overcome by including production and absorptive effects in the production amplitudes.⁴ One then finds that the Froissart bound is saturated from the multiregge region of phase space. This is unsatisfactory experimentally, since particles produced at high energies tend to have rather low relative energies. The region of large relative energies, the multiregge region, is sparsely populated at best. We find that the unitarity condition, properly enforced, produces a new type of cut in the angular momentum place which preserves the Froissart bound and decreases the importance of the multiregge contribution. This unitarity cut is of a dynamical origin which is to be contrasted with the almost kinematical origin of the familiar Mandelstam⁵ and

AFS⁶ cuts. The Mandelstam cuts are also present here. The unitarity cut actually forces the contribution of the multiregge region to decrease at large energies except for rather narrow ranges of the parameters of the theory.

In Section II we present our procedure for constructing unitary models. The input is the amplitude for the production of n particles from a single chain, W_n , shown in Figure 2. For a wide range of input functions it is possible to construct a multiparticle S-matrix that is unitary for all physical values of the total energy.

The essential feature of our procedure is that production from more than one chain is taken into account. Suppose the amplitude W_n is taken from the multiperipheral model and that the elementary particle or Reggeon being exchanged has spin α . Then W_n will have a high energy behavior of the form s^α . On the other hand, amplitudes corresponding to the exchange of N chains will have asymptotic behavior of the form $s^{1+N(\alpha-1)}$, aside from logarithmic factors. Clearly when $\alpha \approx 1$ as in the case of Pomeron exchange, multi-chain exchange is important. As we shall see in specific models, even when α is much less than one, multi-chain effects are important whenever the coupling constant associated with particle production becomes large.

For the models discussed here the standard perturbation expansion of the S-matrix diverges. In fact each S-matrix element has a branch point at zero value of the coupling constant. This divergence is of a general nature and is probably present in many field theories.⁷ Nevertheless it is possible to develop a convergent series expansion for the S-matrix whose form guarantees that unitary is satisfied.

In Section III we consider a specific form for W_n which is based on the multi-peripheral model, but which is simple enough so that every S-matrix element can be written down in closed form. It has two parameters, the coupling constant of the produced mesons and the position of the fixed pole which is exchanged along the multiperipheral chain. The most striking features of this model can be seen by studying the elastic scattering amplitude. This amplitude has contributions from ladder graphs shown in Figure 3a. As in the multiperipheral model, the leading singularity in the angular momentum plane arising from these graphs is a pole. However, the elastic amplitude also has terms arising from checkerboard diagrams of the form shown in Figure 3b. If one sums over all checkerboard graphs with N vertical lines, the leading ℓ -plane singularity is again a pole. In addition, after summing over all N one obtains a square root branch cut in the ℓ -plane. It should be emphasized that this singularity is of a completely different origin than the familiar Mandelstam cut. It arises only after a sum over an infinite number of exchanges. This cut has its origins in the divergence of the sum of the perturbation expansion mentioned above.

For small values of the coupling constant associated with particle production the cut is far to the left of the ℓ -plane, and the leading singularity is the pole arising from the ladder graphs. As the coupling constant is increased the dynamical poles move to the right; however, the branch point moves even faster and overtakes them. As each pole collides with the branch point, it moves through it onto an unphysical sheet. For large enough values of the coupling constant all of the ℓ -plane poles are to the right of one; however, no

pole reaches one before passing on to the unphysical sheet so there is no violation of the Froissart bound. For most values of the parameters in the model the branch point never reaches one. After colliding with the last pole it turns around and retreats towards minus infinity if the coupling constant is increased indefinitely. Nevertheless, for a very restricted range of values for the coupling constant, the leading singularity reaches the point $\ell = 1$. In this case the Froissart bound is saturated. This occurs only if the input pole is itself above 1.

In Section IV we test the generality of the cut mechanism by considering a model in which W_n is essentially the amplitude of the multiperipheral model. In this case the S-matrix elements cannot be written down in closed form. However, after introducing θ -functions into W_n which guarantee that the sub-energies along each chain are large, it is possible to write down an integral equation that sums the checkerboard graphs with N vertical lines. It is then shown that the square root branch cut found in the previous model is also present here and that all singularities in the ℓ -plane to the right of one are on an unphysical sheet. It appears that these properties are far more general than the simple models that we have studied explicitly.

For the models discussed in Sections III and IV it is possible to write down cross sections for particle production in both inclusive and exclusive experiments. These results are also given in Sections III and IV.

In Section V we conclude by briefly summarizing our results.

II. CONSTRUCTION OF THE S-MATRIX

In the present work we shall discuss models with two types of particles. Those whose momenta are labelled by p_a and p_b will be referred to as nucleons although we shall neglect spin and internal quantum numbers. All of the states of interest will contain two nucleons which will be treated as non-identical particles. The S-matrix will be taken to be unity when acting on states with other than two nucleons. The second type of particle, whose momenta are labelled by q_i , will be referred to as pions. The pions can be created and destroyed, and we shall consider states with arbitrary numbers of them. The pions will be treated as identical particles. We take the beam direction to be along the z axis, and write a general four vector q in terms of the transverse momentum, q , which is a two-dimensional vector in the x - y plane; and the longitudinal rapidity, y , defined by

$$y = \frac{1}{2} \ln \left[(q_0 + q_z) / (q_0 - q_z) \right]. \quad (1)$$

Let us start by considering the amplitude, W_n , for the production of n pions from a single chain. This amplitude is shown in Figure 2. A complete set of variables for describing W_n is

$$\begin{aligned} Y &\equiv \ln(s/m^2) \\ \Delta &\equiv \frac{1}{2} (\tilde{p}_a^i - p_a) - \frac{1}{2} (\tilde{p}_b^i - p_b) \end{aligned} \quad (2)$$

and

$$\tilde{q}_i, y_i \quad i = 1, 2, \dots, n.$$

Here m is the nucleon mass and s the square of the center of mass energy.

At high energies Y is the difference of rapidities of the incident nucleons.

From rotational invariance W_n can only depend on the scalar products of Δ and the \tilde{q}_i , so there are just the required $3n + 2$ independent variables.

By crossing symmetry W_n also describes chains in which some or all of the pions are incoming. It is convenient to introduce a single operator which handles all possible processes described by W_n . To this end we introduce creation and annihilation operators for the pions. In our normalization the commutation relations are given by

$$[a(\tilde{q}, y), a^+(\tilde{q}', y')] = 2(2\pi)^3 \delta^2(\tilde{q} - \tilde{q}') \delta(y - y') . \quad (3)$$

Recalling that under crossing $\tilde{q} \rightarrow -\tilde{q}$ and $y \rightarrow y$, we can write the required operator, Z_n , in the form

$$Z_n = \int d^4x \int dp_a dp_b dp'_a dp'_b \sum_{i=1}^n dq_i \cdot \frac{1}{n!} \cdot W_n(Y, \Delta; \tilde{q}_1, y_1 \dots \tilde{q}_n, y_n) | \tilde{p}'_a, y'_a; \tilde{p}'_b, y'_b > < \tilde{p}_a, y_a; \tilde{p}_b, y_b | \cdot e^{ix \cdot (p_a + p_b - p'_a - p'_b)} : \sum_{i=1}^n \left[a(\tilde{q}_i, y_i) e^{iq_i \cdot x} + a^+(-\tilde{q}_i, y_i) e^{-iq_i \cdot x} \right] : \quad (4)$$

Here $|\tilde{p}_a, y_a; \tilde{p}_b, y_b >$ is a two nucleon state, and \tilde{q}_i is the four-vector obtained from q_i by making the substitution $\tilde{q}_i \rightarrow -\tilde{q}_i$. The Lorentz invariant phase space volume is given by $dq = d^2\tilde{q} dy / 2(2\pi)^3$. We have normal ordered the creation and annihilation operators of the pions so that a pion which is emitted from the chain cannot be reabsorbed on it. The important point to notice is

that Z_n is an hermitian operator provided W_n is real and is invariant under a change of sign of all the transverse momenta. These are the two major restrictions which we place on the W_n . Since we wish to consider chains involving an arbitrary number of pions it is convenient to introduce the hermitian operator

$$Z = \sum_{n=0}^{\infty} Z_n . \quad (5)$$

The unitarity of the S-matrix can now be guaranteed by writing^{1,2}

$$S = \sum_{N=0}^{\infty} \frac{i^N}{N!} Z^N = e^{iZ} . \quad (6)$$

What is being said in Eq. (6) is that all of the chains exchanged between the nucleons are uncorrelated except for the constraints imposed by energy-momentum conservation. This is certainly the simplest ansatz that one can make. It is suggested by the relativistic eikonal model¹; however, in this case there is no requirement of straight line propagation for the nucleons.

Eq. (6) provides a convenient definition of the S-matrix when the model is exactly solvable or when the matrix elements of the power series in Z converge. An example is the model of production amplitudes discussed in I. However, in the models to be discussed below the matrix elements of Z^N grow like $\exp(cN^2)$, so the defining series for S diverges rather badly. In such cases it is necessary to use an alternative construction procedure. We first introduce the auxiliary operator $\tilde{S}(z)$ defined by

$$\tilde{S}(z) = \sum_{N=0}^{\infty} \frac{i^N}{N!} Z^N e^{-d^2 N^2} , \quad (7)$$

and then write the S-matrix as

$$S = \frac{1}{\pi^{\frac{1}{2}}} \int_{-\infty}^{\infty} dx e^{-x^2} \tilde{S}(ze^{2dx}) , \quad (8)$$

where d is a parameter chosen so that the sum in Eq. (7) and the integral in Eq. (8) converge. Whenever it is permissible to interchange the order of integration and summation Eqs. (7) and (8) reduce to Eq. (6). Even when this interchange is not possible, Eqs. (7) and (8) define an explicitly unitary S-matrix. To see this notice that formally

$$\tilde{S}(Z) = \frac{1}{\pi^{\frac{1}{2}}} \int_{-\infty}^{\infty} du e^{-u^2} \exp[iZe^{2idu}] , \quad (9)$$

so

$$S^+ S = \frac{1}{\pi^2} \int_{-\infty}^{\infty} dx \int_{-\infty}^{\infty} dx' \int_{-\infty}^{\infty} du \int_{-\infty}^{\infty} du' \exp \left[iZ \left(e^{2d(x+iu)} - e^{2d(x'-iu')} \right) \right] . \quad (10)$$

The right hand side of Eq. (10) has a power series expansion in Z that converges magnificently. One easily sees that the coefficient of Z^N vanishes identically for $N > 1$ and that $S^+ S = S S^+ = 1$. We realize that certain orders of integration have been freely interchanged, but there is no doubt that this new construction procedure is more general than the standard expansion.

Once the W_n are specified the S-matrix is completely determined by Eqs. (4), (5), (7) and (8). The model is clearly broad enough to allow us to investigate a wide range of production and absorption mechanisms. The major problem is to extract the predictions of the model for a particular choice of W_n . For the remainder of this paper we shall be concerned with a particularly

simple class of W_n which is suggested by the relativistic eikonal model. As was mentioned above, the only correlations between the chains are those imposed by energy momentum conservation. These can be greatly simplified by introducing theta functions into the W_n which restrict the range of the pion rapidities. Energy-momentum conservation requires that in the center of mass

$$|y_i| \leq \frac{1}{2} Y + C, \quad (11)$$

where C is a constant which depends on mass ratios. We now introduce the further requirement that the W_n vanish unless

$$|y_i| \leq \frac{1}{2}(1 - \epsilon)Y, \quad (12)$$

where ϵ is an arbitrarily small positive number. At very high energies the restriction of Eq. (12) forces the nucleons to have energies of order $\sqrt{s}/2$, and equal but opposite longitudinal momenta.¹ As long as the average multiplicity does not grow as fast as $s^{\frac{1}{2}\epsilon}$, the pion variables can be dropped from the energy and longitudinal momentum conservation delta functions.¹

It is convenient to introduce the variables

$$\begin{aligned} \tilde{p} &= \tilde{p}_a + \tilde{p}_b \\ \text{and} \quad \tilde{p} &= \frac{1}{2}(\tilde{p}_a - \tilde{p}_b), \end{aligned} \quad (13)$$

and write the two nucleon state of definite total and relative transverse momentum as $|\tilde{p}, \tilde{p}; y_a, y_b\rangle$. Eq. (4) now becomes

$$\begin{aligned}
 Z_n \simeq \int dp_a dp_b \frac{d^2 p'}{(2\pi)^2} \prod_{i=1}^n dq_i \frac{1}{n!} \\
 \cdot \frac{1}{2s} W_n(Y, \Delta; \tilde{q}_i, y_i) | \tilde{p} - \sum_1^n \tilde{q}_i, \tilde{p}'; y_a, y_b > < \tilde{p}, \tilde{p}; y_a, y_b | \\
 : \prod_{i=1}^n \left[a(\tilde{q}_i, y_i) + a^+(-\tilde{q}_i, y_i) \right] : . \quad (14)
 \end{aligned}$$

At this point it is useful to introduce the co-ordinate, \tilde{B} , conjugate to \tilde{p} . \tilde{B} can be interpreted as the transverse distance between the nucleons. Defining the two nucleon state of definite \tilde{B} by

$$| \tilde{p}, \tilde{B}; y_a, y_b > = \int \frac{d^2 p}{(2\pi)^2} e^{-i\tilde{B} \cdot \tilde{p}} | \tilde{p}, \tilde{p}; y_a, y_b > , \quad (15)$$

Eq. (14)-becomes

$$\begin{aligned}
 Z_n \simeq \int d^2 b \frac{d^2 p}{(2\pi)^2} \frac{dy_a}{4\pi} \frac{dy_b}{4\pi} \prod_{i=1}^n dq_i \frac{1}{n!} \\
 \cdot \frac{1}{2s} W_n(Y, B; \tilde{q}_i, y_i) | \tilde{p} - \sum \tilde{q}_i, B; y_a, y_b > < \tilde{p}, B; y_a, y_b | \\
 : \prod_{i=1}^n \left[a(\tilde{q}_i, y_i) + a^+(-\tilde{q}_i, y_i) \right] : , \quad (16)
 \end{aligned}$$

where

$$W_n(Y, B; \tilde{q}_i, y_i) = \int \frac{d^2 \Delta}{(2\pi)^2} e^{i\Delta \cdot B} W_n(Y, \Delta; \tilde{q}_i, y_i) . \quad (17)$$

Clearly the S-matrix is diagonal in \tilde{B} .

At this stage the only function of the two nucleon projection operator is to give rise to the energy-momentum conservation delta function. We factor this delta function out of the problem, and then introduce the reduced operator

$$Z_n(Y, \tilde{B}) = \frac{1}{2s} \frac{1}{n!} \int \prod_{i=1}^n dq_i W_n(Y, \tilde{B}; \tilde{q}_i, y_i) : \prod_{i=1}^n \left[q(\tilde{q}_i, y_i) + a^+(-\tilde{q}_i, y_i) \right] : \quad (18)$$

Operators $Z(Y, \tilde{B})$ and $S(Y, \tilde{B})$ can be obtained from $Z_n(Y, \tilde{B})$ in direct analogy with Eqs. (5), (7) and (8). It is also useful to introduce a scattering amplitude operator defined by

$$M(Y, \tilde{\Delta}) = \int d^2 B e^{-i\Delta \cdot B} Z(Y, \tilde{B}) = 2is \int d^2 B e^{-i\Delta \cdot B} [1 - S(Y, \tilde{B})]. \quad (19)$$

Clearly these operators act in the Hilbert space spanned by the pion states. The only reference to the nucleon states that remains is in the diagonal variables Y and \tilde{B} . This reduction of the Hilbert space can only take place exactly in eikonal models. It should be emphasized that although the restrictions of Eq. (12) provide a simplification, they are by no means necessary for the construction of unitary models.

III. A SOLVABLE MODEL

In order to illustrate our ideas we now construct a solvable model. Although this model is highly simplified, its solution contains most of the qualitative features of the more sophisticated model discussed in Section IV.

In defining W_n we follow the spirit of the multiperipheral model to the extent that we order the rapidities along the chain. We take the exchange mechanism between adjacent particles on the chain to be that of a fixed pole. Working in the center of mass we write

$$\frac{1}{2s} W_n(Y, B; \tilde{q}_i, y_i) = e^{-Y} f(B) \prod_{i=0}^n e^{\alpha(y_i - y_{i+1})} \theta(y_i - y_{i+1}) \cdot \prod_{j=1}^n g(\tilde{q}_j), \quad (20)$$

where $y_0 = -y_{n+1} = \frac{1}{2} Y$. The crucial simplification which allows us to solve the model in closed form is the neglect of all correlations involving the transverse momenta of the pions. Of course this cannot be justified experimentally. However, we shall be primarily interested in the energy dependence of this model. Since the transverse momenta are limited, a fact which we build into the function $g(\tilde{q})$, it is hoped that their correlations do not play too strong a role in determining the dependence of the amplitudes on the total energy.⁸

From rotational invariance $g(\tilde{q})$ must be a function of \tilde{q}^2 . Then making use of the symmetry of W_n as a function of the pion momenta, we find

$$\begin{aligned} Z_n(Y, B) &= f(B) e^{(\alpha-1)Y} \frac{1}{n!} \\ &: \prod_{i=1}^n \int \frac{d^2 \tilde{q}_i}{(2\pi)^2} \int_{-\frac{1}{2}(1-\epsilon)Y}^{\frac{1}{2}(1-\epsilon)Y} \frac{dy_i}{4\pi} g(\tilde{q}_i) \left[a(\tilde{q}_i, y_i) + a^+(\tilde{q}_i, y_i) \right] : \end{aligned} \quad (21)$$

It is convenient to introduce the annihilation operator

$$c = [\lambda Y]^{-\frac{1}{2}} \int \frac{d^2 \tilde{q}}{(2\pi)^2} J_{-\frac{1}{2}(1-\epsilon)Y}^{\frac{1}{2}(1-\epsilon)Y} \frac{dy}{4\pi} g(\tilde{q}) a(\tilde{q}, y), \quad (22)$$

with

$$\lambda_0 = \frac{1}{4\pi} \int \frac{d^2 \tilde{q}}{(2\pi)^2} g(\tilde{q})^2 \equiv \lambda/(1-\epsilon). \quad (23)$$

Clearly c and c^+ satisfy the usual harmonic oscillator commutation relations

$$[c, c^+] = 1. \quad (24)$$

The operator $Z(Y, B)$ is given by

$$\begin{aligned} Z(Y, B) &= \sum_{n=0}^{\infty} Z_n(Y, B) \\ &= f(B) e^{(\alpha-1)Y} : e^{(\lambda Y)^{\frac{1}{2}}(c+c^+)} : \\ &= f(B) e^{(\alpha-1-\frac{1}{2}\lambda)Y} e^{(2\lambda Y)^{\frac{1}{2}}x}. \end{aligned} \quad (25)$$

In the last step we have introduced the hermitian "coordinate" operator

$x = \frac{1}{\sqrt{2}}(c + c^+)$. The S-matrix operator $S(Y, B) = e^{iZ(Y, B)}$, is obviously diagonal in the coordinate representation.

Let us start by considering elastic scattering of the two nucleons where the matrix element of $S(Y, B)$ between states with no pions must be evaluated. In the coordinate representation this is just familiar ground state wave function of the harmonic oscillator:

$$\begin{aligned}
 < 0 | \underset{\sim}{S}(Y, B) | 0 > &= \underset{\sim}{S}_{22}(Y, B) \\
 &= \frac{1}{\sqrt{\pi}} \int_{-\infty}^{\infty} dx e^{-x^2} \exp \left[i f(\underset{\sim}{B}) e^{Y(\alpha - 1 - \frac{1}{2}\lambda)} e^{(2\lambda Y)^{\frac{1}{2}}x} \right] \\
 &= (2\lambda Y)^{-\frac{1}{2}} \exp \left[-Y(1 - \alpha + \frac{1}{2}\lambda)^2 / 2\lambda \right] \frac{1}{\sqrt{\pi}} \int_0^{\infty} dr r \\
 &\quad \cdot \exp \left[-\ln r (1 - \alpha + \frac{1}{2}\lambda) / \lambda - (\ln r)^2 / 2\lambda Y + i f(\underset{\sim}{B}) r \right]. \tag{26}
 \end{aligned}$$

We can study the ℓ -plane structure of the elastic scattering amplitude by making use of Eq. (19) and taking the Laplace transform with respect to Y :⁹

$$\begin{aligned}
 M_{22}(\ell, B) &= \int_0^{\infty} dY e^{-\ell Y} M_{22}(Y, B) \\
 &= 2im^2 \left[2\lambda(\ell - \alpha_c) \right]^{-\frac{1}{2}} \left[\int_0^{\infty} dr r^{(2/\lambda)^{\frac{1}{2}} \left[(\ell - \alpha_c)^{\frac{1}{2}} - (1 - \alpha_c)^{\frac{1}{2}} \right] - 1} \left(1 - e^{i f(\underset{\sim}{B}) r} \right) \right. \\
 &\quad \left. + \int_1^{\infty} dr r^{(2/\lambda)^{\frac{1}{2}} \left[-(\ell - \alpha_c)^{\frac{1}{2}} - (1 - \alpha_c)^{\frac{1}{2}} \right] - 1} \left(1 - e^{i f(\underset{\sim}{B}) r} \right) \right]. \tag{27}
 \end{aligned}$$

where

$$\alpha_c = 1 - (1 - \alpha + \frac{1}{2}\lambda)^2 / 2\lambda = \alpha - \frac{(1 - \alpha - \frac{1}{2}\lambda)^2}{2\lambda}. \tag{28}$$

For the case $\alpha \leq 1 + \frac{1}{2}\lambda$, we have

$$\begin{aligned}
 M_{22}(\ell, B) &= 2im^2 \left\{ 1/(\ell - 1) - \left[2\lambda(\ell - \alpha_c) \right]^{-\frac{1}{2}} \left[-i f(\underset{\sim}{B}) \right]^{(2/\lambda)^{\frac{1}{2}} \left[(1 - \alpha_c)^{\frac{1}{2}} - (\ell - \alpha_c)^{\frac{1}{2}} \right]} \right. \\
 &\quad \left. \cdot \Gamma \left[(2/\lambda)^{\frac{1}{2}} \left((\ell - \alpha_c)^{\frac{1}{2}} - (1 - \alpha_c)^{\frac{1}{2}} \right) \right] \right\} + C(\ell, B), \tag{29}
 \end{aligned}$$

where $C(\ell, B)$ is an entire function of ℓ for all values of B . $M_{22}(\ell, B)$ clearly has poles in the ℓ -plane at

$$\alpha(N) = 1 + N(\alpha-1) + \frac{1}{2}\lambda N(N-1) \quad N = 1, 2, \dots \quad (30)$$

with residues

$$\beta(N) = -2i\pi^2 \left[\text{if}_{\tilde{B}}(B) \right]^N / N! \quad (31)$$

Notice that each power of $f(B)$ corresponds to the exchange of one chain. The $N = 1$ pole arises from the exchange of a single fixed input pole. The $N = 2$ pole arises from the ladder graphs and the poles with $N \geq 3$ from the checkerboard graphs with N vertical lines.

In addition to the poles there is a fixed square root branch point at $\ell = \alpha_c$. The associated cut runs along the negative real axis from $-\infty$ to α_c . It is clear from Eq. (29) that the only poles on the physical sheet are those for which $'\alpha(N) - \alpha_c'$ is positive. These are the poles for which

$$N \leq \bar{N} = (1 - \alpha + \frac{1}{2}\lambda)/\lambda , \quad (32)$$

where \bar{N} is the value of N which produces a minimum of $\alpha(N)$ as a function of N .

Let us imagine increasing λ from zero to infinity for a fixed value of $\alpha \leq 1$. For small values of λ the branch point is far to the left in the ℓ -plane. As λ is increased all of the dynamical poles move to the right, but the branch point moves to the right even faster. The left-most pole on the physical sheet collides with the branch point whenever λ is such that \bar{N} is an integer since

$$\alpha(N) = 1 - (1 - \alpha + \frac{1}{2}\lambda)^2/2\lambda = \alpha_c . \quad (33)$$

After colliding with the branch point the poles moves off onto the unphysical sheets as λ is increased further. At $\lambda = 2(1 - \alpha)$, the branch point circles around the pole at $\alpha(1) = \alpha$ and then starts to retreat down the negative real axis. For $\lambda > 2(1 - \alpha)$, the branch point is the only singularity of M_{22} on the

physical sheet. Notice that for large values of λ all of the dynamical poles are to the right of $\ell = 1$; however, any pole that reaches $\ell = 1$ is on the unphysical sheet.

For $\alpha(2) \geq \alpha_c$, that is $\lambda < \frac{2}{3}(1 - \alpha)$, the pole from the ladder graphs controls the high energy behavior of the total cross section and

$$\sigma_T(s) \xrightarrow[s \rightarrow \infty]{} (s/m^2)^{2(\alpha-1) + \lambda} \int d^2 \tilde{B} [f(\tilde{B})]^2. \quad (34)$$

However for $\alpha_c > \alpha(2)$, or $\lambda > \frac{2}{3}(1 - \alpha)$, one has

$$\sigma_T(s) \xrightarrow[s \rightarrow \infty]{} \frac{(s/m^2)^{\alpha_c-1}}{[\ln(s/m^2)]^{\frac{1}{2}}} \frac{(\pi/2\lambda)^{\frac{1}{2}}}{\sin\left[\frac{\pi}{2} \left[(1 - \alpha_c)\frac{2}{\lambda}\right]^{\frac{1}{2}}\right] \Gamma\left[1 + \left[(1 - \alpha_c)\frac{2}{\lambda}\right]^{\frac{1}{2}}\right]} \cdot \int d^2 \tilde{B} [f(\tilde{B})]^{\left[(1 - \alpha_c)\frac{2}{\lambda}\right]^{\frac{1}{2}}}. \quad (35)$$

Note that if the fixed input pole has spin $\alpha \leq 1 + \frac{1}{2}\lambda$, the total cross section goes to zero asymptotically. In particular, for $\alpha = 1$, we have for all values of the coupling constant

$$\sigma_T(s) \xrightarrow[s \rightarrow \infty]{} \frac{(s/m^2)^{-\lambda/8}}{[\ln(s/m^2)]^{\frac{1}{2}}} 2\lambda^{-\frac{1}{2}} \int d^2 \tilde{B} [f(\tilde{B})]^{\frac{1}{2}}. \quad (36)$$

Now let us consider what happens if α is increased for a fixed value of λ . As mentioned above, for $\alpha > 1 - \frac{1}{2}\lambda$, the branch point at α_c is the only singularity on the physical sheet. α_c reaches 1 when $\alpha = 1 + \frac{1}{2}\lambda$. At this point the total cross section falls like $[\ln(s/m^2)]^{-\frac{1}{2}}$ at large energies. As α circles the point $1 + \frac{1}{2}\lambda$ we move from the positive to the negative branch of $(1 - \alpha_c)^{\frac{1}{2}}$.

The function $C(\ell, \tilde{B})$ defined in Eq. (29) then develops a singularity. Returning to Eq. (27), $M_{22}(\ell, \tilde{B})$ can now be written in the form

$$M_{22}(\ell, \tilde{B}) = 2im^2(\ell-1)^{-1} \left[-if(\tilde{B}) \right]^{(2/\lambda)^{\frac{1}{2}} \left[(\ell-\alpha_c)^{\frac{1}{2}} + (1-\alpha_c)^{\frac{1}{2}} \right]} + C'(\ell, \tilde{B}), \quad (37)$$

where the only singularity of $C'(\ell, \tilde{B})$ is the branch point at $\ell = \alpha_c$.

It is instructive at this point to consider a particular choice for $f(\tilde{B})$. Choosing $f(\tilde{B}) = e^{-B/R}$ and taking the Fourier transform with respect to \tilde{B} gives

$$M_{22}(\ell, \Delta) = 2im^2 R_0^2 \left[(\ell-1)^2 + R_0^2 \Delta^2 \right]^{-3/2} + C''(\ell, \Delta) \quad (38)$$

where

$$R_0 = R(\alpha - 1 - \frac{1}{2}\lambda), \quad (39)$$

and C'' has only the branch point at $\ell = \alpha_c$. The first term in Eq. (38) is just the ℓ -plane singularity corresponding to the scattering from a black disc of radius R_0 . It gives rise to a total cross section of the form²

$$\sigma_T(s) \xrightarrow[s \rightarrow \infty]{} 2\pi R_0^2 \left[\ln(s/m^2) \right]^2. \quad (40)$$

The complex conjugate branch points of Eq. (38) enter the physical sheet through the square root cut when $\alpha_c = 1$, i. e. when $\alpha = 1 + \frac{1}{2}\lambda$. As α is increased further the radius of the black disc increases according to Eq. (39) and α_c decreases. It is amusing that the Froissart bound can only be saturated for a rather limited range of the parameters. If α is now held fixed, and λ is increased, R_0 shrinks to zero at $\lambda = 2(\alpha-1)$. For $\lambda > 2(\alpha-1)$ the branch point at α_c is again the only singularity of M_{22} . So, for λ large enough the total cross section always vanishes at infinite energy.

In preparation for the more sophisticated model to be discussed in Section IV, it is instructive to consider the series expansion of $S(Y, \tilde{B})$ in powers of $Z(Y, \tilde{B})$. Since

$$\langle 0 | Z(Y, \tilde{B})^N | 0 \rangle = \frac{1}{N!} f(\tilde{B})^N e^{Y[N(\alpha-1) + \frac{1}{2}\lambda N(N-1)]}, \quad (41)$$

the series expansion for $S(Y, \tilde{B})$ given in Eq. (6) diverges. In fact if we write $f(\tilde{B}) = G \bar{f}(\tilde{B})$, the S-matrix has a branch point as a function of G at $G = 0$. On the other hand, it is possible to choose the parameter d so that the series for \tilde{S}_{22} is well defined:

$$\langle 0 | \tilde{S}(Z) | 0 \rangle = \sum_{n=0}^{\infty} \frac{[if(\tilde{B})]^N}{N!} e^{Y[N(\alpha-1) + \frac{1}{2}\lambda N(N-1)]} e^{-d^2 N^2}. \quad (42)$$

The most convenient choice is $d = (\frac{1}{2}\lambda Y)^{\frac{1}{2}}$. Then

$$\langle 0 | \tilde{S}(Z) | 0 \rangle = \exp \left[if(\tilde{B}) e^{Y(\alpha-1-\frac{1}{2}\lambda)} \right], \quad (43)$$

and Eq. (26) follows immediately from Eq. (8).

We conclude this section by briefly considering production processes. The inclusive cross section for the production of a single pion by two incident nucleons is

$$\begin{aligned}
 \frac{d\sigma}{d^2\mathbf{q} dy} &= \frac{1}{2(2\pi)^3} d^2 B \sum_{n=0}^{\infty} \int \prod_{i=1}^n dq_i \frac{1}{n!} \langle \mathbf{q}, y; \mathbf{q}_1, y_1; \dots, \mathbf{q}_n, y_n | S(Y, B) | 0 \rangle^2 \\
 &= \frac{1}{2(2\pi)^3} \int d^3 B \langle 0 | [S^+(Y, B), a^+(\mathbf{q}, y)] [S(Y, B), a(\mathbf{q}, y)] | 0 \rangle \\
 &= \frac{1}{2(2\pi)^3} \int d^3 B \langle 0 | [Z(Y, B), a^+(\mathbf{q}, y)] S^+ S \cdot [a(\mathbf{q}, y), Z(Y, B)] | 0 \rangle \\
 &= \frac{1}{2(2\pi)^3} g(\mathbf{q})^2 \int d^2 B \langle 0 | Z(Y, B)^2 | 0 \rangle.
 \end{aligned} \tag{44}$$

Thus the single particle inclusive distribution is determined by the ladder graphs independent of whether the pole arising from these graphs is on the physical sheet or not. All contributions to the inclusive cross section arising from the checkerboard graphs have cancelled.

If $\lambda \leq \frac{2}{3}(1-\alpha)$ the situation is more complicated. First consider the case $\alpha \leq 1$. The total cross section is now dominated at high energies by the branch point at $\ell = \alpha_c$. From Eqs. (35) and (41) we see that the average multiplicity is now given by

$$\bar{n} = C(s/m^2)^{[2(\alpha-1) + \lambda + (1-\alpha_c)]} [\ln(s/m^2)]^{3/2}, \tag{46}$$

where C is a constant. In Section II we mentioned that the type of model presently being considered is internally consistent only if \bar{n} grows less rapidly than $s^{\frac{1}{2}\epsilon}$. Since ϵ must lie between zero and one, λ is restricted to

$$\lambda \leq \frac{2}{9} \left[(4-3\alpha) + (7-6\alpha)^{\frac{1}{2}} \right], \quad \alpha \leq 1. \tag{47}$$

The equality holds for $\epsilon = 1$ at which point λ_0 is infinite. Thus, although the effective coupling constant, λ , is limited in range, the "real" coupling constant λ_0 can take on any value between zero and infinity.

For $\alpha > 1$ and $\lambda < 2(\alpha-1)$ the total cross section is given by Eq. (40) and the multiplicity by

$$\bar{n} = C' (s/m^2)^{2\alpha-2+\lambda} [\ln(s/m^2)]^{-1}. \quad (48)$$

Clearly we must require that $\alpha \leq 5/4$ and $\lambda \leq 5/2-2\alpha$. Finally, for $\alpha > 1$ and $\lambda \geq 2(\alpha-1)$, \bar{n} is again given by Eq. (46). The restriction of Eq. (47) still holds with the further requirement that $\alpha \leq 9/8$.

The restrictions on λ and α are rather artificial. They arise only because we have insisted on simplifying the model by dropping the pion variables from the energy and longitudinal momentum conservation delta functions, as discussed in Section II.

The exclusive cross section for the production of n pions is given by

$$\sigma_n(Y) = \frac{1}{n!} \int d^2 B \prod_{i=1}^n dq_i | \langle \tilde{q}_1, y_1; \dots, \tilde{q}_n, y_n | S | 0 \rangle |^2. \quad (49)$$

The production amplitude can be written in the form

$$\langle \tilde{q}_1, y_1; \dots, \tilde{q}_n, y_n | S | 0 \rangle = \prod_{i=1}^n g(q_i) A_n(Y, B), \quad (50)$$

with

$$\begin{aligned}
 A_n(Y, \tilde{B}) &= (2\lambda Y)^{-n/2} \frac{1}{\sqrt{\pi}} \int_{-\infty}^{\infty} dx e^{-x^2} H_n(x) \tilde{S}(x) \\
 &= (2\lambda Y)^{-(n-1)/2} \frac{1}{\sqrt{\pi}} \int_{-\infty}^{\infty} dx e^{-x^2} H_{n-1}(x) \tilde{S}(x) \cdot \text{if}(\tilde{B}) e^{[(\alpha-1-\frac{1}{2}\lambda)Y + (2\lambda Y)^{\frac{1}{2}}x]}.
 \end{aligned} \tag{51}$$

$H_n(x)$ is the Hermite polynomial of order n and

$$\tilde{S}(x) = \exp \left[\text{if}(\tilde{B}) e^{[(\alpha-1-\frac{1}{2}\lambda)Y + (2\lambda Y)^{\frac{1}{2}}x]} \right]. \tag{52}$$

Clearly the pions are produced independently. Furthermore, the production amplitude is independent of the rapidities of the pions, so that

$$\sigma_n(Y) = \frac{1}{n!} \int d^2 \tilde{B} |A_n(Y, \tilde{B})|^2 (\lambda Y)^n. \tag{53}$$

For $\lambda \leq \frac{2}{3}(1-\alpha)$, the only important contributions to the high energy production amplitudes come from diagrams in which all pions are produced from a single chain. In this case one sees from Eq. (51) that

$$A_n(Y, B) \simeq \text{if}(B) e^{Y(\alpha-1)}, \tag{54}$$

and

$$\sigma_n(s) \xrightarrow[s \rightarrow \infty]{} (s/m^2)^{2(\alpha-1)} [\lambda \ln(s/m^2)]^n \frac{1}{n!} \int d^2 \tilde{B} [f(\tilde{B})]^2. \tag{55}$$

Since these are the same graphs that are considered in the multiperipheral model, the poisson distribution is hardly surprising.

For those values of α and λ for which the square root branch point dominates the total cross section the situation is more complicated. For

$\lambda \leq 2(1-\alpha)$ and $n \ll Y$ Eqs. (54) and (55) still hold. On the other hand, for $\lambda > 2(1-\alpha)$ we see from Eq. (51) that

$$A_n(Y, B) \simeq -e^{(\alpha_c - 1)Y} (2\lambda Y)^{-n/2} H_{n-1} \left[(1 - \alpha_c)^{\frac{1}{2}} Y^{\frac{1}{2}} \right] \left[-i f(B) \right]^{(1 + \frac{1}{2}\lambda - \alpha)/\lambda} \Gamma(\frac{1}{2}\lambda + \alpha - 1) \quad (56)$$

for $n \ll Y$ and $\alpha < 1 + \frac{1}{2}\lambda$. For $n \gtrsim Y$ the explicit expression for σ_n is rather involved and we shall not write it down. It is clear, however, that the pion distribution is not Poisson. Similarly, the pion distribution deviates markedly from a Poisson distribution for the case of black disc scattering. It is left as an exercise for the reader to show that for all values of λ and α the identity

$$\sum_{n=0}^{\infty} \sigma_n(s) = \sigma_T(s) \quad (57)$$

follows directly from Eq. (51).

IV. A MULTI-PERIPHERAL MODEL

In this section we shall discuss a form for W_n which is based on the multi-peripheral or multiregge model. Ideally one would like to take W_n to be the ordinary multi-peripheral amplitude and define the S-matrix via Eqs. (4), (7) and (8). This program is technically difficult, but not impossible. We hope to return to it at a later time. For the present we shall consider a slightly simplified form for W_n which correctly reproduces the multi-peripheral amplitude for large values of the sub-energies. This is an interesting region since it is the large sub-energy tails that lead to difficulty with the Froissart bound in the ordinary multi-peripheral model and saturate that bound in improved treatments.³ Our main aim here is to show how these terms can add up to give a small, energy decreasing contribution to the total cross section in the present model. We shall see that the cut mechanism discussed in section III operates here also.

We again impose the restriction on the pion rapidities given in Eq. (12). This has the effect of guaranteeing that the first and last sub-energies along each chain are large. It is convenient to introduce the variables (see figure 2)

$$\tilde{k}_i = - \sum_{j=0}^{i-1} \tilde{q}_j = \sum_{j=i}^{n+1} \tilde{q}_j$$

(58)

$$x_i = y_{i-1} - y_i ,$$

where

$$\begin{aligned} q_0 &= \tilde{p}_a' - \tilde{p}_a, & q_{n+1} &= \tilde{p}_b' - \tilde{p}_b \\ \text{and} \\ y_0 &= -y_{n+1} = \frac{1}{2} Y. \end{aligned} \tag{59}$$

We then write the amplitude W_n as

$$W_n(Y, \Delta; q_1, y_1; \dots q_n, y_n) = \prod_{i=1}^{n+1} \beta(\tilde{k}_i) e^{\alpha(\tilde{k}_i) \tilde{x}_i} \theta(x_i) \cdot \prod_{j=1}^n g(\tilde{k}_j, \tilde{k}_{j+1}). \quad (60)$$

$\alpha(\tilde{k})$ and $\beta(\tilde{k})$ are the trajectory and residue functions of the Regge pole exchanged between adjacent particles along the chain.¹⁰ One factor of the vertex function g is to be associated with the creation or destruction of each pion. As was mentioned above, the amplitude for W_n coincides with the multiperipheral amplitude only when all the sub-energies are large. Only then are all the momentum transfers transverse and all the rapidities strongly ordered.

Expressions for the operators $Z(Y, B)$ and $M(Y, \Delta)$ can now be read off from Eqs. (17) - (19). We start by considering the elastic scattering amplitude. The first step is to calculate the matrix elements of Z^N between states with no pions. Let us define

$$Z_N(Y, \Delta) = \int d^2 \tilde{B} e^{-i \tilde{\Delta} \cdot \tilde{B}} \langle 0 | Z(Y, B)^N | 0 \rangle. \quad (61)$$

Then the contribution from the exchange of a single chain is just the familiar Regge pole amplitude,

$$Z_1(Y, \Delta) = (2m^2)^{-1} \beta(\Delta) e^{Y[\alpha(\Delta)-1]} \quad (62)$$

The terms of second order in $Z(Y, B)$ give rise to the ladder graphs of figure 3a. We have

$$\begin{aligned}
 Z_2(Y, \Delta) &= \sum_{n=0}^{\infty} Z_2^n(Y, \Delta) \\
 &= \sum_{n=0}^{\infty} (2s)^{-2} \int d^2 B e^{-i\Delta \cdot B} \int_{i=1}^n \prod_{i=1}^n dq_i \\
 &\quad \cdot W_n(Y, B; q_1, y_1; \dots; q_n, y_n) W_n(Y, B; -q_1, y_1; \dots; -q_n, y_n) \\
 &= \sum_{n=0}^{\infty} (2s)^{-2} \int_{i=1}^{n+1} \prod_{i=1}^{n+1} \frac{dk_i}{(2\pi)^2} \frac{dx_i}{4\pi} \cdot 4\pi \delta \left(\sum_{i=1}^{\infty} x_i - Y \right) \\
 &\quad \cdot \prod_{i=1}^{n+1} \beta(k_i) \beta(\Delta + k_i) e^{x_i [\alpha(k_i) + \alpha(\Delta + k_i)]} \\
 &\quad \prod_{j=1}^n g(k_j, k_{j+1}) g(\Delta + k_j, \Delta + k_{j+1}) \tag{63}
 \end{aligned}$$

Eq. (63) is simplified by taking the Laplace transform with respect to Y :

$$\begin{aligned}
 Z_2^n(\ell, \Delta) &\equiv \int_0^{\infty} dY e^{-\ell Y} Z_2^n(Y, \Delta) \\
 &= (2m^2)^{-2} \int_{i=1}^{n+1} \prod_{i=1}^{n+1} \frac{dk_i}{(2\pi)^2} \beta(k_i) \beta(\Delta + k_i) [\ell - \alpha(k_i) - \alpha(\Delta + k_i) + 2]^{-1} \\
 &\quad \cdot \prod_{j=1}^n (4\pi)^{-1} g(k_j, k_{j+1}) g(\Delta + k_j, \Delta + k_{j+1}). \tag{64}
 \end{aligned}$$

The sum in Eq. (63) is the solution to an integral equation which is completely analogous to the Lippman-Schwinger equation in two-dimensions.¹¹ To see this in detail, and for later use, the free Green's function for the propagation of two Reggeons is defined by

$$\begin{aligned} \langle \tilde{k}_1' \tilde{k}_2' | G_2(\ell) | \tilde{k}_1 \tilde{k}_2 \rangle &= (2\pi)^4 \delta^2(\tilde{k}_1 - \tilde{k}_1') \delta^2(\tilde{k}_2 - \tilde{k}_2') \\ &\cdot [\alpha(\tilde{k}_1) + \alpha(\tilde{k}_2) - \ell - 2]^{-1}, \end{aligned} \quad (65)$$

and the potential between two Reggeons by

$$\begin{aligned} \langle \tilde{k}_1' \tilde{k}_2' | V_{12} | \tilde{k}_1 \tilde{k}_2 \rangle &= - (2\pi)^2 \delta^2(\tilde{k}_1 + \tilde{k}_2 - \tilde{k}_1' - \tilde{k}_2') \\ &\cdot [\beta(\tilde{k}_1) \beta(\tilde{k}_2) \beta(\tilde{k}_1') \beta(\tilde{k}_2')]^{\frac{1}{2}} (4\pi)^{-1} g(\tilde{k}_1, \tilde{k}_2) g(\tilde{k}_1', \tilde{k}_2'). \end{aligned} \quad (66)$$

The full Green's function, $g_2(\ell)$, satisfies the operator equation

$$g_2(\ell) = G_2(\ell) + G_2(\ell) V_{12} g_2(\ell). \quad (67)$$

Now $Z_2(\ell, \Delta)$ is obtained from $g_2(\ell)$ via the equation

$$(2\pi)^2 \delta^2(\Delta - \Delta') Z_2(\ell, \Delta) = - (2m^2)^{-2} \langle F_2(\Delta') | g_2(\ell) | F_2(\Delta) \rangle, \quad (68)$$

where

$$\langle \tilde{k}_1 \tilde{k}_2 | F(\Delta) \rangle = (2\pi)^2 \delta^2(\tilde{k}_1 + \tilde{k}_2 - \Delta) [\beta(\tilde{k}_1) \beta(\tilde{k}_2)]^{\frac{1}{2}}. \quad (69)$$

The analogy with the Lippman-Schwinger equations becomes exact if we take the input trajectories to be linear:

$$\alpha(\tilde{k}) = \alpha - \alpha' \tilde{k}^2. \quad (70)$$

The "free Hamiltonian" is then

$$H_0 = \alpha' \tilde{k}_1^2 + \alpha' \tilde{k}_2^2. \quad (71)$$

and the quantity $E_2 \equiv -\ell + 2(\alpha - 1)$ plays the role of energy. Notice that as long as the functions $\beta(\tilde{k})$ and $g(\tilde{k}, \tilde{k}')$ have no zeroes, the potential is purely attractive. As a result, for strong enough coupling there will always be bound states, i.e., Regge poles.

As is well known, the integral equation for the ladder graphs simplifies considerably if the vertex function, g , is taken to be a constant. In this case the potential is separable and we have

$$Z_2(\ell, \Delta) = J(\ell, \Delta) \left[1 - \frac{g^2}{4\pi} J(\ell, \Delta) \right]^{-1}, \quad (72)$$

where

$$J(\ell, \Delta) = \int \frac{d^2 \tilde{k}}{(2\pi)^2} \beta(\tilde{k} + \frac{1}{2}\Delta) \beta(\tilde{k} - \frac{1}{2}\Delta) [\ell - 2(\alpha - 1) + 2\alpha' \tilde{k}^2 + \frac{1}{2}\alpha' \Delta^2]^{-1}. \quad (73)$$

As ℓ increases from $2(\alpha - 1) - \frac{1}{2}\alpha' \Delta^2$, $J(\ell, \Delta)$ decreases monotonically. There is obviously a single Regge pole to the right of the branch point at $\ell = 2(\alpha - 1) - \frac{1}{2}\alpha' \Delta^2$. Since the separable approximation does not appreciably simplify the general checkerboard diagrams, we shall retain the dependence of the vertex functions on the transverse momenta.

Integral equations for the checkerboard graphs with N vertical lines can be written down in analogy with the one for the ladder graphs. There is one new complication here. For $N \leq 3$ the fact that the rapidities are ordered along each chain implies that the rapidities of all particles in the intermediate states are ordered. This is not true for $N \geq 4$ as can be seen by considering the

simple example shown in figure 4. Any diagram for which the rapidity order is not completely determined can be written as a sum of terms, each of which does have a definite rapidity ordering. If we consider each of these terms to be a distinct diagram, then there is a one to one correspondence between our diagrams and those of non-relativistic potential scattering. The rapidity variables play a role analogous to that of the time variable in ordinary quantum mechanics.

Proceeding as in the case of the ladder graphs, we introduce a free Green's function for the propagation of N Reggeons,

$$\begin{aligned} \langle \tilde{k}_1', \dots \tilde{k}_N' | G_N(\ell) | \tilde{k}_1, \dots \tilde{k}_N \rangle &= \prod_{i=1}^N (2\pi)^2 \delta^2(\tilde{k}_i - \tilde{k}_i') \\ &\quad [\sum_{i=1}^N \alpha(k_i) - \ell - N]^{-1}. \end{aligned} \tag{74}$$

The N -Reggeon potential is written as

$$V_N = \sum_{i < j}^N V_{ij}, \tag{75}$$

where

$$\begin{aligned} \langle \tilde{k}_1' \dots \tilde{k}_N' | V_{ij} | \tilde{k}_1, \dots \tilde{k}_N \rangle &= - \prod_{m \neq i, j} (2\pi)^2 \delta^2(\tilde{k}_m - \tilde{k}_m') \\ &\quad \cdot (2\pi)^2 \delta^2(\tilde{k}_i + \tilde{k}_j - \tilde{k}_i' - \tilde{k}_j') [\beta(\tilde{k}_i) \beta(\tilde{k}_j) \beta(\tilde{k}_i') \beta(\tilde{k}_j')]^{1/2} \\ &\quad \cdot (4\pi)^{-1} g(\tilde{k}_i, \tilde{k}_j) g(\tilde{k}_i', \tilde{k}_j'). \end{aligned} \tag{76}$$

The full Green's function $g_N(\ell)$ is determined from the integral equation

$$g_N(\ell) = G_N(\ell) + G_N(\ell) V_N g_N(\ell), \quad (77)$$

and $Z_N(\ell, \Delta)$ is given by

$$(2\pi)^2 \delta^2(\Delta - \Delta') Z_N(\ell, \Delta) = - (2m^2)^{-N} \langle F_N(\Delta') | g_N(\ell) | F_N(\Delta) \rangle, \quad (79)$$

where

$$\begin{aligned} \langle \tilde{k}_1, \dots, \tilde{k}_N | F_N(\Delta) \rangle &= (2\pi)^2 \delta^2 \left(\sum_{i=1}^N \tilde{k}_i + \Delta \right) \\ &\cdot \prod_{i=1}^N [\beta(k_i)]^{\frac{1}{2}} \\ &\equiv (2\pi)^2 \delta^2 \left(\sum_{i=1}^N \tilde{k}_i + \Delta \right) \langle \tilde{k}_1 \dots \tilde{k}_N | f_N(\Delta) \rangle. \end{aligned} \quad (79)$$

Clearly, obtaining $g_N(\ell)$ is equivalent to solving the N -body Schroedinger equation in two-dimensions. We are most interested in the leading behavior of $Z_N(Y, \Delta)$ for large Y , or, in other words, in the right-most singularity of $g_N(\ell)$ in the ℓ -plane. If there were no bound states, this singularity would be the N -Reggeon Mandelstam cut. However, in general we expect discrete bound state poles since the potential is attractive.

Using the linear trajectory defined in Eq. (70), we introduce the N -Reggeon free Hamiltonian

$$H_{0N} = \sum_{i=1}^N \alpha' \tilde{k}_i^2 \quad (80)$$

The Green's function $g_N(\ell)$ will have poles for those values of ℓ for which there are solutions to the eigenvalue equation

$$H_N |\Psi_N(\Delta)\rangle = [H_{0N} + V_N] |\Psi_N(\Delta)\rangle = E_N |\Psi_N(\Delta)\rangle, \quad (81)$$

with

$$E_N \equiv -\ell + N(\alpha - 1). \quad (82)$$

The two-Reggeon potentials V_{ij} are well behaved at the origin and at infinity.

We therefore expect that in the ground state of the N-Reggeon system, the kinetic energy will increase like N and the potential energy will decrease like $-\frac{1}{2}N(N-1)$, the number of pairwise Reggeon potentials. In the appendix we obtain upper and lower bounds on the ground state energy E_N^0 . For a wide class of input functions $\beta(k)$ and $g(k, k')$, E_N^0 does indeed decrease $-\frac{1}{2}N(N-1)$ for large N . Denoting the leading trajectory function arising from the checkerboard graphs with N vertical lines by $\alpha_N(\Delta)$, we write¹²

$$\alpha_N(0) = a(N) - Nb + N^2 c \equiv \alpha_N^0. \quad (83)$$

The results of the appendix show that c is a positive number and that $[a(N) - Nb]/N^2$ goes to zero for large N . If α_N has neither a branch point nor an essential singularity at $N = \infty$, then b can be chosen so that $a(N)$ goes to a constant for large N .

Denoting the contribution to $Z_N(Y, \Delta)$ arising from the leading Regge pole by $Z_N^P(Y, \Delta)$ we write

$$Z_N^P(Y, \Delta) = \beta_N(\Delta) e^{Y[\alpha_N(\Delta) - 1]} \quad (84)$$

In the appendix it is shown that for a wide range of inputs $\beta_N(\Delta)$ is bounded by β_0^N/N , where β_0 is a constant. It is further argued that $\alpha'_N(0) \equiv \alpha'_N$ goes to a constant at large N .¹³ Our final results do not depend strongly on the precise form of $\beta_N(\Delta)$.

The crucial result is Eq. (83). Since $Z_N(\ell, \Delta)$ has poles arbitrarily far to the right in the ℓ -plane, it is clear that the series expansion for $S(Y, B)$ given in Eq. (6) can not converge. However, since $S(Y, B)$ is unitary, $S_{22}(Y, B)$ is bounded by one for all Y and B . As a result, all of the poles in $Z_N(\ell, \Delta)$ to the right of $\ell=0$ must be on an unphysical sheet of the ℓ -plane.¹² To see how the branch cut arises in the present model, let us perform the sometimes risky operation of summing the contributions of the leaping poles in $Z_N(Y, \Delta)$. First, Eq. (84) will be rewritten in the form

$$Z_N^P(Y, \Delta) = (N+1)^{-1} C_N(\Delta) \beta_0^N e^{Y[a(N) - bN + cN^2 - \alpha'_N \Delta^2 - 1]}, \quad (85)$$

where we have made a linear expansion in Δ^2 for the trajectory function. The results of the appendix imply that $a(N)$, α'_N and $C_N(\Delta)$ all bounded by constants for large N .⁷

$Z_N^P(Y, \Delta)$ has contributions only from diagrams in which all N Reggeons interact, in other words only from connected graphs. Now the elastic S-matrix element, or rather its phase, is given by

$$i\chi(Y, B) \equiv \ln [S_{22}(Y, \beta)] = [S_{22}^C(Y, \beta) - 1], \quad (86)$$

where the superscript c means that S_{22} is computed by including only connected diagrams. From Eqs. (7) and (8) we see that the contribution of the pole terms

to χ , using Eqs. 8 and 85, is

$$\begin{aligned}
 i\chi^P(Y, \Delta) &= \frac{1}{\pi^{\frac{1}{2}}} \int_{-\infty}^{\infty} dx e^{-x^2} \sum_{N=1}^{\infty} \frac{i^N}{(N+1)!} C_N(\Delta) \\
 &\quad \cdot e^{Y[a(N) - 1 - \alpha'_N \Delta^2]} \left[\beta_0 e^{-bY} e^{2(cY)^{\frac{1}{2}}x} \right]^N \\
 &\equiv \frac{1}{\pi^{\frac{1}{2}}} \int_{-\infty}^{\infty} e^{-x^2} i\chi^P(x). \tag{87}
 \end{aligned}$$

In writing Eq. (87) we have taken $d = (cY)^{\frac{1}{2}}$.

The asymptotic behavior of $\chi^P(Y, \Delta)$ can be read off directly from Eq. (87).⁸ The integrand has quite different behavior depending on whether x is larger or smaller than $x_0 = bY^{\frac{1}{2}}/2c^{\frac{1}{2}}$. For $x \leq x_0$ we can integrate the series term by term. Writing

$$I_1 = \frac{1}{\pi^{\frac{1}{2}}} \int_{-\infty}^{x_0} e^{-x^2} i\chi^P(x) = \sum_{N=1}^{\infty} I_1(N), \tag{88}$$

we see that for large Y

$$\begin{aligned}
 I_1(N) &\simeq \frac{i^N}{N!} \beta_N(\Delta) e^{Y[\alpha'_N(\Delta) - 1]} \\
 &\quad \left[\theta(b/2c - N) - \frac{e^{-cY(b/2c - N)^2}}{2\pi(cY)^{\frac{1}{2}}(b/2c - N)} \right]. \tag{89}
 \end{aligned}$$

On the other hand for $x > x_0$ we can not integrate the series term by term. If $C_N(\Delta)$, $a(N)$ and α'_N are analytic functions of N in the right half N -plane and do

not have a branch point or essential singularity at infinity we have^{13,15}

$$\begin{aligned}
 L_2 &= \frac{1}{\pi^{\frac{1}{2}}} \int_{x_0}^{\infty} dx e^{-x^2} i\chi P(x) \\
 &\simeq C_{\infty}(\Delta) e^{Y[a(\infty) - 1 - \alpha_{\infty} \Delta^2]} \frac{1}{\pi^{\frac{1}{2}}} \int_{x_0}^{\infty} dx e^{-x^2} \exp[i\beta_0 e^{-bY + 2(cY)^{\frac{1}{2}}x}] \\
 &\cdot [i\beta_0 e^{-bY + 2(cY)^{\frac{1}{2}}x}]^{-1} \\
 &- C_0(\Delta) e^{Y[a(0) - 1 - \alpha_0' \Delta^2]} \frac{1}{\pi^{\frac{1}{2}}} \int_{x_0}^{\infty} dx e^{-x^2} \\
 &\simeq Y^{-\frac{1}{2}} e^{-Yb^2/4c} [K_{\infty}(\Delta) e^{Y[a(\infty) - 1 - \alpha_{\infty}' \Delta^2]} \\
 &- K_0(\Delta) e^{Y[a(0) - 1 - \alpha_0' \Delta^2]}] . \tag{90}
 \end{aligned}$$

In the present approximation, the elastic scattering amplitude is given by

$$M_{22}(Y, \Delta) = 2is \int d^2 B e^{-i\Delta \cdot B} \frac{i\chi P(Y, B)}{[1 - e^{-i\Delta \cdot B}]} . \tag{91}$$

From Eq. (89) we see that as in the case of the solvable model there are only a finite number of Regge poles on the physical sheet of the ℓ -plane. One new feature is that there are an infinite number of square root branch points with $\Delta^2 = 0$ intercepts at

$$\alpha_c(N) = a(N) - b^2/4c . \tag{92}$$

In order to study the movement of the poles and branch points in the ℓ -plane, it is convenient to introduce an effective pion coupling constant by writing $g(\underline{k}, \underline{k}') = \lambda^{\frac{1}{2}} g'(\underline{k}, \underline{k}')$. Applying Feynman's theorem to the eigenvalues of

Eq. (81) for large values of N , we see that c is a monotonically increasing function of λ . Let us concentrate on the case of forward scattering. From the results of the appendix we know that there exists an integer $N_0(\lambda)$ such that $Z_N(\ell, 0)$ has a pole on the physical sheet for all $N \geq N_0(\lambda)$. As λ is increased from zero this pole can enter the physical sheet through the normal threshold branch point associated with the scattering of N free Reggeons. This branch point is located at $\ell = N(\alpha - 1)$. Alternatively the pole could enter the physical sheet through a branch point associated with the scattering of compound systems made up of a total of N -Reggeons, or through an anomalous threshold. However, for small values of λ , these branch points are arbitrarily close to the point $\ell = N(\alpha - 1)$. As a result,

$$\begin{aligned} c &\xrightarrow[\lambda \rightarrow 0]{} 0 \\ b &\xrightarrow[\lambda \rightarrow 0]{} 1 - \alpha \end{aligned} \tag{93}$$

Let us start by considering values of the input parameters for which $b > 0$. For small values of λ we see from Eqs. (89) and (90) that the branch points of $M_{22}(\ell, \Delta)$ are arbitrarily far to the left. Those Regge poles for which $N \leq b/2c$ are on the physical sheet. As λ is increased we know from Feynman's theorem on derivatives of eigenvalues that the poles move to the right in the ℓ -plane. We also expect the branch points to move to the right. Whenever a pole collides with its corresponding cut, the pole moves on to an unphysical sheet. For large values of λ we expect from our counting argument that the potential energy decreases like $-cN(N - 1)$. We therefore write $b = b' + c$. Although we can really say nothing about the behavior of b' , it would appear to

be an accident if it approached the value $-c$ for large λ . We therefore expect the branch points to turn around and retreat towards minus infinity if λ is made large enough. If b' does not grow as rapidly as c with increasing λ , then there will be no poles on the physical sheet for sufficiently large values of λ and the total cross section will go to zero at high energies.

In the solvable model discussed earlier, $a(N) \equiv 1$. In the present case we can say nothing about the function $a(N)$ without further calculation. In particular we can not rule out the possibility of $a(N)$ becoming large enough so that

$\chi^P(\ell, \Delta)$ has poles or cuts to the right of $\ell = 0$. If this occurs then $S_{22}(Y, B)$ will vanish for B inside a disc whose radius grows like $\ln(s/m^2)$. As is well known this behavior for $S_{22}(Y, B)$ leads to a saturation of the Froissart bound.

The ℓ -plane structure of the elastic amplitude is as given in Eq. (38).

Finally let us imagine varying the input parameters so that b decreases through zero. For negative values of b the elastic scattering amplitude has no poles on the physical sheet. If $a(N) > 1$ for any value of N , we again have saturation of the Froissart bound when $b = 0$. However, if the magnitude of b becomes sufficiently large, the complex conjugate branch points of Eq. (38) will leave the physical sheet through a square root branch point as in the solvable model. The total cross section will then go to zero once again. If $a(N) \leq 1$ for all N then the square root branch points are the only singularities on the physical sheet of the ℓ -plane for negative values of b .

Consider the problem of including non-leading contributions to $Z_N(Y, \Delta)$. The series for \tilde{S}_{22} will certainly converge with $d = (cY)^{\frac{1}{2}}$. Furthermore, in the integral over x from minus infinity to x_0 , one can again interchange the order of integration and summation. The only change is to include lower order poles and branch points in the ℓ -plane. The real problem is to study the integral from x_0

to infinity; this is difficult to do explicitly, but it is hard to see how the basic structure of the amplitude could be altered.

The exclusive and inclusive single particle production cross sections can be treated as in the solvable model. Using the relation

$$[a(b, y), Z(Y, B)] = g Z(\frac{1}{2}Y - y, \frac{1}{2}B + b) Z(\frac{1}{2}Y + y, \Delta = 0). \quad (94)$$

which holds if $g(k, k')$ is a constant, it is a straightforward matter to write down these cross sections. The rapidity distribution is particularly simple in the inclusive case.

$$\frac{d\sigma}{dy} = \frac{g^2}{4\pi} Z_2(\frac{1}{2}Y - y, \Delta = 0) Z_2(\frac{1}{2}Y + y, \Delta = 0). \quad (95)$$

which shows that the ladder graphs determine the inclusive distribution just as in the previous model, Eq. (44). The exclusive cross section is more complicated because the precise form of the eigenvalue spectrum $\alpha_N(\Delta)$ must be used. The final result does not seem to be particularly illuminating.

ACKNOWLEDGMENT

We wish to thank H. M. Fried and H. D. I. Abarbanel for very helpful discussions.

V. SUMMARY

The point we wish to emphasize is that the mechanism for avoiding violation and saturation of the Froissart bound discussed in these solvable models is available in more general theories. In any unitary relativistic theory which does not exhibit saturation of forces, that is, in which the binding in the exchange channel grows faster than $N \ln N$, where N is the number of exchanged quanta, the unitarity cut must develop. Since the amplitudes $Z_N(\ell, \Delta)$ then have poles arbitrarily far to the right in the ℓ -plane, this cut must arise to preserve unitarity. In the models discussed here, the binding energy of the ground state grows as N^2 , which follows from the fact that the number of pairwise interactions grows as $N(N - 1)/2$. It is difficult to see how a similar result could fail to hold in more sophisticated models where low sub-energy effects are taken into account. Since the S matrix is unitary, the elastic scattering amplitude is forbidden to have any ℓ -plane poles to the right of one on the physical sheet. As a result it must have branch cuts in the ℓ -plane which have been exhibited in our models and which are of a different type than those discussed by Mandelstam.⁴ For the solvable model we find that if the input trajectory is 1 or below, the multiregge region provides a contribution to the total cross section which decreases as a power of the energy. Hence the experimentally observed constant total cross sections must arise from other sources, such as the fragmentation region or the low sub-energy pionization region.

APPENDIX

In this appendix we obtain the bounds on the trajectory and residue functions that were employed in the text. We start by obtaining upper and lower bounds on the ground state energy, E_N^0 , for the Hamiltonian of Eq. (81). An upper bound is obtained from the Rayleigh-Ritz variational principle. We use a separable trial function

$$\langle \tilde{k}_1 \cdots \tilde{k}_N | \psi_N^T \rangle = \prod_{i=1}^N f(\tilde{k}_i), \quad (A-1)$$

where

$$\int \frac{d^2 \tilde{k}}{(2\pi)^2} |f(\tilde{k})|^2 = 1. \quad (A-2)$$

Then

$$E_N^0 \leq N I - \frac{1}{2} N(N-1) J \quad (A-3)$$

with

$$I = \int \frac{d^2 \tilde{k}}{(2\pi)^2} |f(\tilde{k})|^2 \tilde{k}^2 \quad (A-4)$$

and

$$\begin{aligned} J = & \int \frac{d^2 \tilde{k}}{(2\pi)^2} \frac{d^2 \tilde{k}_2}{(2\pi)^2} \frac{d^2 \tilde{k}_1'}{(2\pi)^2} \frac{d^2 \tilde{k}_2'}{(2\pi)^2} (2\pi)^2 \delta^2(\tilde{k}_1 + \tilde{k}_2 - \tilde{k}_1' - \tilde{k}_2') \\ & \cdot [\beta(\tilde{k}_1) \beta(\tilde{k}_2) \beta(\tilde{k}_1') \beta(\tilde{k}_2')]^{\frac{1}{2}} (4\pi)^{-1} g(\tilde{k}_1, \tilde{k}_1') g(\tilde{k}_2, \tilde{k}_2') \\ & \cdot f(\tilde{k}_1) f(\tilde{k}_2) f^*(\tilde{k}_1') f^*(\tilde{k}_2'). \end{aligned} \quad (A-5)$$

We require that $\beta(\tilde{k})$ and $g(\tilde{k}, \tilde{k}')$ have no zeroes and that $g(\tilde{k}, \tilde{k}')$ is a symmetric function of its arguments. As a result, I and J are positive definite quantities.

In order to obtain a lower bound on E_N^0 , it is convenient to write the exact wave function in the form

$$\langle \tilde{k}_1, \dots, \tilde{k}_N | \Psi_N(\Delta) \rangle = (2\pi)^2 \delta^2(\sum \tilde{k}_i + \Delta) \psi_N(\tilde{k}_1, \dots, \tilde{k}_N), \quad (A-6)$$

with ψ_N normalized to

$$\langle \psi_N | \psi_N \rangle \equiv \int_{i=1}^N \frac{d^2 \tilde{k}_i}{(2\pi)^2} (2\pi)^2 \delta^2(\sum \tilde{k}_i + \Delta) |\psi_N(\tilde{k}_1, \dots, \tilde{k}_N)|^2 = 1 \quad (A-7)$$

Then

$$\begin{aligned} E_N^0 &= \langle \psi_N | H_{ON} + V_N | \psi_N \rangle \\ &\geq \langle \psi_N | V_N | \psi_N \rangle = \frac{1}{2}N(N-1) \langle \psi_N | V_{12} | \psi_N \rangle. \end{aligned} \quad (A-8)$$

In the last step we have used the fact that $\psi_N(\tilde{k}_1, \dots, \tilde{k}_N)$ is a symmetric function of its arguments.

Introducing the variables

$$\begin{aligned} \tilde{K} &= \tilde{k}_1 + \tilde{k}_2 \\ \tilde{k} &= \frac{1}{2}(\tilde{k}_1 - \tilde{k}_2) \end{aligned} \quad (A-9)$$

we have

$$\begin{aligned} E_N^0 &\geq -\frac{1}{2}N(N-1) \int_{i=3}^N \frac{d^2 \tilde{k}_i}{(2\pi)^2} \frac{d^2 \tilde{K}}{(2\pi)^2} \frac{d^2 \tilde{k}}{(2\pi)^2} \frac{d^2 \tilde{k}'}{(2\pi)^2} \\ &\cdot (2\pi)^2 \delta^2(\tilde{K} + \sum_{i=3}^N \tilde{k}_i + \Delta) \psi_N(\tilde{K}, \tilde{k}, \tilde{k}_3, \dots, \tilde{k}_N) \psi_N^*(\tilde{K}, \tilde{k}, \tilde{k}_3, \dots, \tilde{k}_N) \\ &\cdot [\beta(\frac{1}{2}\tilde{K} + \tilde{k}) \beta(\frac{1}{2}\tilde{K} - \tilde{k}) \beta(\frac{1}{2}\tilde{K} + \tilde{k}') \beta(\frac{1}{2}\tilde{K} - \tilde{k}')] \\ &\cdot (4\pi)^{-1} g(\frac{1}{2}\tilde{K} + \tilde{k}, \frac{1}{2}\tilde{K} + \tilde{k}') g(\frac{1}{2}\tilde{K} - \tilde{k}, \frac{1}{2}\tilde{K} - \tilde{k}'). \end{aligned} \quad (A-10)$$

Making use of the Schwartz inequality we see that

$$E_N^0 \geq -\frac{1}{2}N(N-1) \int_{i=1}^N \frac{d^2 \tilde{k}_i}{(2\pi)^2} (2\pi)^2 \delta^2 \left(\sum_{i=1}^N \tilde{k}_i + \Delta \right) | \psi_N(\tilde{k}_1, \dots, \tilde{k}_N) |^2 L(\tilde{k}) \quad (A-11)$$

$$| \psi_N(\tilde{k}_1, \dots, \tilde{k}_N) |^2 L(\tilde{k})$$

where

$$L(\tilde{k})^2 = \int \frac{d^2 \tilde{k}}{(2\pi)^2} \frac{d^2 \tilde{k}'}{(2\pi)^2} \beta(\frac{1}{2}\tilde{k} + \tilde{k}) \beta(\frac{1}{2}\tilde{k} - \tilde{k}) \beta(\frac{1}{2}\tilde{k} + \tilde{k}') \beta(\frac{1}{2}\tilde{k} - \tilde{k}') (4\pi)^{-2} g^2(\frac{1}{2}\tilde{k} + \tilde{k}, \frac{1}{2}\tilde{k} + \tilde{k}') g^2(\frac{1}{2}\tilde{k} - \tilde{k}, \frac{1}{2}\tilde{k} - \tilde{k}') \quad (A-12)$$

The only requirements that we have made on β and g so far is that they have no zeroes and that they are well enough behaved so that all the integrals converge. We now impose the further requirement that there exists a finite L such that $L \geq L(\tilde{k})$ for all \tilde{k} . This is a very mild restriction. For example, we certainly expect that g is bounded for all values of its argument. Denoting its upper bound by g_m , we have

$$L(\tilde{k}) \leq \frac{g_m^2}{4\pi} \int \frac{d^2 \tilde{k}}{(2\pi)^2} \beta(\frac{1}{2}\tilde{k} + \tilde{k}) \beta(\frac{1}{2}\tilde{k} - \tilde{k}) . \quad (A-13)$$

The right hand side of Eq. (A-13) can be bounded by a constant for a wide range of β 's. From Eqs. (A-7) and (A-11) we now have

$$-\frac{1}{2}N(N-1)J + NI \geq E_N^0 \geq -\frac{1}{2}N(N-1)L. \quad (A-14)$$

Eq. (83) now follows directly from Eqs. (A-14) and (82).

The slope of the leading trajectory is more difficult to estimate. If the potential, V_N , were Galilean invariant, then the only dependence of $g_N(\ell)$ on the total transverse momentum would be through the free Green's functions.

In that case we would have the exact result

$$\alpha_N(\Delta) = A_N - \alpha' \Delta^2/N. \quad (A-15)$$

However, V_N can be Galilean invariant only if we choose β to be a constant and take $g(\mathbf{k}, \mathbf{k}') = g(\mathbf{k} - \mathbf{k}')$, a rather unlikely parameterization. In the general case the slope of the trajectory function $\alpha_N(\Delta)$ will be effected by the Δ dependence of the potentials. Writing the momenta \mathbf{k}_i in terms of Δ and momenta relative to the center of mass, we see that Δ always enters the V_{ij} in the form Δ/N . From our simple counting argument we expect $\alpha'_N(0)$ to go like a constant at large N . This is the assumption made in the text. It is by no means crucial to our argument.

Finally we obtain a bound on the residue function, $\beta_N(\Delta)$, where

$$\beta_N(\Delta) = |\langle \psi_N | f_N(\Delta) \rangle|^2, \quad (A-16)$$

and $|f_N(\Delta)\rangle$ is defined in Eq. (79). Using the Schwartz inequality we see that

$$\begin{aligned} \beta_N(\Delta) &\leq |\langle f_N(\Delta) | f_N(\Delta) \rangle| \\ &= \int \prod_{i=1}^N \frac{d^2 \tilde{\mathbf{k}}_i}{(2\pi)^2} (2\pi)^2 \delta^2 \left(\sum_{i=1}^N \tilde{\mathbf{k}}_i + \Delta \right) \prod_{i=1}^N \beta(\tilde{\mathbf{k}}_i) \\ &= \int d^2 b [\tilde{\beta}(b)]_0^N e^{-i\Delta \cdot b} \end{aligned} \quad (A-17)$$

where $\tilde{\beta}(\mathbf{b})$ is the two-dimensional Fourier transform of $\beta(\mathbf{k})$. One easily verifies that for most simple parameterizations of $\beta(\mathbf{k})$, $\beta_N(\Delta)$ can be bounded by a function of the form β_0^N/N , where β_0 is a constant. For example, if we write $\beta(\mathbf{k}) = \beta_0 e^{-k^2/\mu^2}$, then

$$\langle f_N(\Delta) | f_N(\Delta) \rangle = (4/N\mu^2) (\beta_0 \pi \mu^2)^N e^{-\Delta^2/N\mu^2} \quad (A-18)$$

REFERENCES

1. R. Aviv, R. Blankenbecler and R. L. Sugar, UCSB preprint, hereafter referred to as I.
2. Similar models have been discussed by G. Calucci, R. Jengo and C. Rebbi, *Nuovo Cimento* 4A, 330 (1971), 6A, 601 (1971), and to be published. See also the work of L. B. Redei, CERN preprint TH. 1454, Feb. 1972.
3. J. Finkelstein and K. Kajantie, *Phys. Letters* 26B, 305 (1968).
4. H. Cheng and T. T. Wu, *Phys. Rev. Letters* 25, 1586 (1970); J. Finkelstein and F. Zachariasen, *Phys. Letters* 34B, 631 (1971); J. R. Fulco and R. L. Sugar, *Phys. Rev.* D5, 1919 (1971).
5. S. Mandelstam, *Nuovo Cimento* 30, 1113, 1127 and 1143 (1963).
6. D. Amati, A. Stanghellini, and S. Fubini, *Nuovo Cimento* 26, 896 (1962).
7. F. Dyson, *Phys. Rev.* 85, 631 (1952). See also A. M. Jaffe, *Commun. Math. Phys.* 1, 127 (1965), and references therein.
8. This choice for W_n is similar in spirit to the one dimensional models of C. de Tar, *Phys. Rev.* D3, 128 (1971). This author of course only considers the exchange of a single chain in his production amplitudes.
9. A. Erdelyi, et al., *Tables of Integral Transforms*, Vol. I, p. 146.
10. Notice that in order for the S-matrix to be unitary, W_n and therefore β must be real. As a result the input trajectory must be taken to be exchange degenerate.
11. This type of Reggeon calculus is in the spirit of that discussed by V. N. Gribov, *Zh. Eksp. Teor. Fiz.* 53, 654 (1967) [Sov. Physics JETP 26, 414 (1966)] and H. D. I. Abarbanel, NAL Preprint Thy-28 (1972).

12. Because of our normalization the poles in $Z_N(\ell, \Delta)$ are one unit to the left of the corresponding poles in the elastic scattering amplitude, $M_{22}(\ell, \Delta)$. We denote by $\alpha_N(\Delta)$ the position of the poles in $M_{22}(\ell, \Delta)$.
13. In order to simplify our calculations we shall assume that $\alpha_N(\Delta)$ and $\beta_N(\Delta)$ are analytic in the right half N plane and do not have branch points at $N = -\infty$. However, in order to insure that the square root branch points in the ℓ -plane exist it is really sufficient to have $\alpha_N(\Delta)$ increase like N^2 for large N .
14. The interested reader can use the same technique to obtain the high energy behavior of the solvable model discussed in section III.
15. "Studies on Divergent Series and Summability", W. B. Ford, Chelsea Publishing Co., 1916, p. 263.

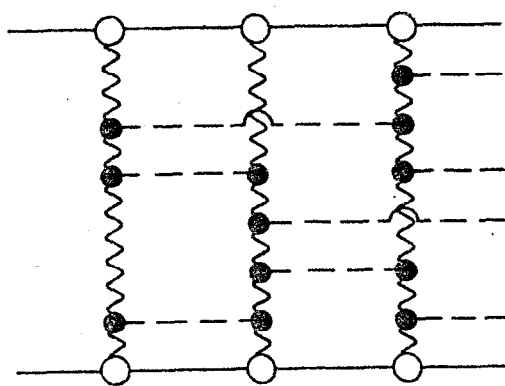
FIGURE CAPTIONS

Figure 1 : General Production Graph

Figure 2: Basic Form of W_n

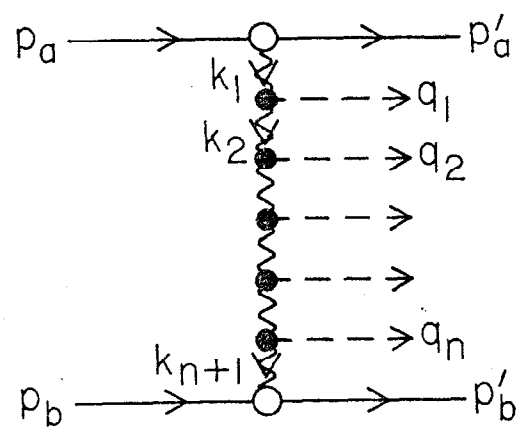
Figure 3: Elastic Ladder (a) and Checkerboard (b) Graphs

Figure 4: Rapidity Orderings



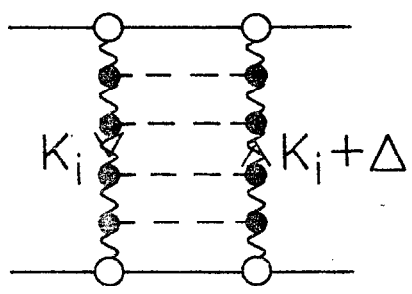
2079A1

Fig. 1

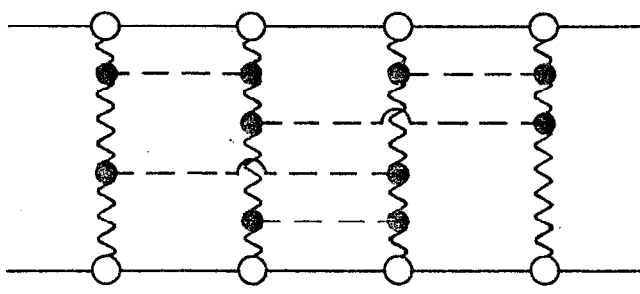


2079A2

Fig. 2



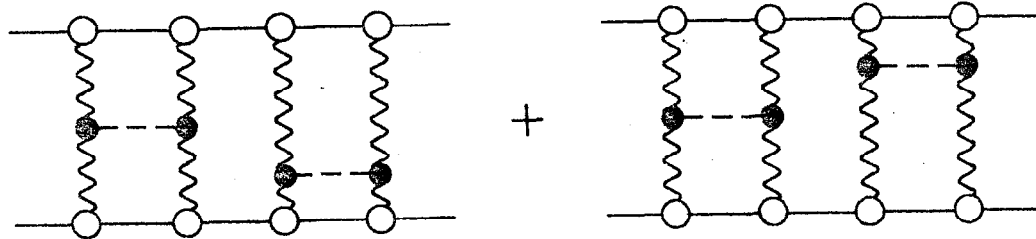
(a)



(b)

2079A3

Fig. 3



2079A4

Fig. 4